Mineralogical Magazine, December 2016, Vol. 80(7), pp. 1265–1272

Gajardoite, $KCa_{0.5}As_4^{3+}O_6Cl_2 \cdot 5H_2O$, a new mineral related to lucabindiite and torrecillasite from the Torrecillas mine, Iquique Province, Chile

ANTHONY R. KAMPF[1,*], BARBARA P. NASH[2], MAURIZIO DINI[3] AND ARTURO A. MOLINA DONOSO[4]

[1] Mineral Sciences Department, Natural History Museum of Los Angeles County, 900 Exposition Boulevard, Los Angeles, CA 90007, USA
[2] Department of Geology and Geophysics, University of Utah, Salt Lake City, Utah 84112, USA
[3] Pasaje San Agustin 4045, La Serena, Chile
[4] Los Algarrobos 2986, Iquique, Chile

[*Received 27 September 2015; Accepted 24 November 2015; Associate Editor: Andrew Christy*]

ABSTRACT

The new mineral gajardoite (IMA2015-040), $KCa_{0.5}As_4^{3+}O_6Cl_2 \cdot 5H_2O$, was found at the Torrecillas mine, Iquique Province, Chile, where it occurs as a secondary alteration phase in association with native arsenic, arsenolite, chongite, talmessite and torrecillasite. Gajardoite occurs as hexagonal plates up to ~100 μm in diameter and 5 μm thick, in rosette-like subparallel intergrowths. Crystals are transparent, with vitreous lustre and white streak. The Mohs hardness is ~1½, tenacity is brittle and fracture is irregular. Cleavage is perfect on {001}. The measured density is 2.64 g/cm^3 and the calculated density is 2.676 g/cm^3. Optically, gajardoite is uniaxial (–) with $\omega = 1.780(3)$ and $\varepsilon = 1.570(5)$ (measured in white light). The mineral is very slowly soluble in H_2O and slowly soluble in dilute HCl at room temperature. The empirical formula, determined from electron-microprobe analyses, is $(K_{0.77}Ca_{0.71}Na_{0.05}Mg_{0.05})_{\Sigma 1.58}As_4O_{11}Cl_{1.96}H_{9.62}$. Gajardoite is hexagonal, *P*6/*mmm*, $a = 5.2558(8)$, $c = 15.9666(18)$ Å, $V = 381.96(13)$ Å^3 and $Z = 1$. The eight strongest powder X-ray diffraction lines are [d_{obs} Å(*I*)(*hkl*)]: 16.00(100)(001), 5.31(48)(003), 3.466 (31)(103), 3.013(44)(104), 2.624(51)(006,110,111), 2.353(36)(113), 1.8647(21)(116,205) and 1.4605(17) (119,303,216). The structure, refined to $R_1 = 3.49\%$ for 169 $F_o > 4\sigma F$ reflections, contains two types of layers. One layer of formula $KAs_4^{3+}O_6Cl_2$ consists of two neutral As_2O_3 sheets, between which are K^+ cations and on the outside of which are Cl^- anions. This layer is topologically identical to a slice of the lucabindiite structure and similar to a slice of the torrecillasite structure. The second layer consists of an edge-sharing sheet of $Ca(H_2O)_6$ trigonal pyramids with isolated H_2O groups centred in the hexagonal cavities in the sheet.

KEYWORDS: gajardoite, new mineral, arsenite, crystal structure, lucabindiite, torrecillasite, Torrecillas mine, Chile.

Introduction

THE Torrecillas mine, in the northern Atacama Desert of Chile, is a small, long-inactive arsenic mine probably discovered and first mined during the guano mining boom of the early 19th century (Mortimer, *et al.*, 1971). It was clearly never a significant producer and was probably finally abandoned several years prior to 1950 (Pimentel, 1978). In recent years, our investigations on the minerals of this unusual deposit have yielded many new and potentially new mineral species. To date, the descriptions of four new minerals have been published: leverettite (Kampf *et al.*, 2013*a*), magnesiokoritnigite (Kampf *et al.*, 2013*b*), torrecillasite (Kampf *et al.*, 2014*a*) and canutite (Kampf *et al.*,

*E-mail: akampf@nhm.org
DOI: 10.1180/minmag.2016.080.065

2014*b*). Herein, we describe the new mineral gajardoite and, in an accompanying paper, we describe the associated new mineral chongite (Kampf *et al*., 2016; IMA2015-039). Several other potentially new minerals are currently under study.

The new mineral gajardoite (/ga: ′ha:r dOu ait/) honours Dr. Anibal Gajardo Cubillos (b. 1945). Dr. Gajardo is a Chilean geologist with a long and distinguished career. He has more than 200 publications, including books, journal papers and conference abstracts and professional reports. These have been principally on the non-metallic mineral deposits of Chile, including those in the Atacama Desert region. He has held several leadership positions in SERNAGEOMIN, Chile's National Geology and Mining Service, most recently (2012–2014) serving as Head of the Geological Hazards and Land Management Unit. He held full- and part-time professorships in the Department of Geology at the University of Chile from 1979 to 2009. He has served as Vice-President and President of the Association of Geologists of Chile, and is a Fellow of the Institute of Mining Engineers of Chile and the Geological Society of Chile. Dr. Gajardo has agreed to the naming of this mineral in his honour.

The new mineral and the name have been approved by the International Mineralogical Association (IMA2015-040, Kampf *et al*., 2015). The description is based upon one holotype and two cotype specimens that are deposited in the collections of the Natural History Museum of Los Angeles County, 900 Exposition Boulevard, Los Angeles, CA 90007, USA, catalogue numbers 65585, 65586 and 65587, respectively. These are the same as the holotype and cotypes for chongite.

Occurrence

The Torrecillas mine is located on Torrecillas Hill, Iquique Province, Tarapacá Region, Chile (approximately 20°58′13″S, 70°8′17″W). Four different rock units are exposed on the hill. The Coastal Range Batholith (mainly gabbros) extends from the seashore to the Pan-American Road along the base of Torrecillas Hill. At the foot of Torrecillas Hill is a small area of contact metamorphic rocks in which garnet crystals occur in metamorphosed shales. Higher on the hill, the rocks are predominantly andesites and porphyritic lavas of the Jurassic La Negra Formation. The Torrecillas deposit, in which the new mineral is found, consists of two main veins rich in secondary arsenic and copper minerals that intersect metamorphosed marine shales and lavas. These mineralized veins are related genetically to the aforementioned andesites and porphyritic lavas of the Jurassic La Negra Formation. More information on the geology and mineralogy of the area is provided by Gutiérrez (1975).

The rare secondary chlorides, arsenates and arsenites have been found at three main sites on the hill: an upper pit measuring ∼8 m long and 3 m deep, a lower pit ∼100 m from the upper pit and measuring ∼5 m long and 3 m deep, and a mine shaft adjacent to the lower pit and lower on the hill. Gajardoite was found in February of 2014 by a collecting party consisting of three of the authors (ARK, MD and AAMD), along with Jochen Schlüter and Joe Marty, at a small excavation a few metres above the shaft.

The new mineral is a secondary alteration phase occurring in association with native arsenic, arsenolite, chongite, talmessite and torrecillasite (Kampf *et al*., 2014*a*). The secondary assemblages at the Torrecillas deposit are interpreted as having formed from the oxidation of native arsenic and other As-bearing primary phases, followed by later alteration by saline fluids derived from evaporating meteoric water under hyperarid conditions (*c.f.* Cameron *et al*., 2007).

We have also confirmed the occurrence of a polytype of gajardoite, gajardoite-3*R* [space group *R*3 with a = 15.759(2) and c = 47.780(3) Å], at a small deposit ∼9 km NE of the village of Cuya in the Camarones Valley, Arica Province, Chile. This deposit was referred to by Kampf *et al*. (2013*c*) as the Cuya NE9 arsenite occurrence.

Physical and optical properties

Gajardoite occurs as hexagonal plates, flattened on {001} and bounded by {100}, up to ∼100 μm in diameter and 5 μm thick, in rosette-like subparallel intergrowths (Figs 1 and 2). No twinning was observed. Crystals are transparent, with vitreous lustre and white streak. The mineral does not fluoresce in longwave or shortwave ultraviolet light. The Mohs hardness is ∼1½ based on scratch tests. The tenacity is brittle and the fracture is irregular. Cleavage is perfect on {001}. The density measured by flotation in sodium polytungstate solution is 2.64(2) g/cm^3 and the calculated density based on the empirical formula is 2.676 g/cm^3. The mineral is very slowly soluble in H_2O and slowly soluble in dilute HCl at room temperature. Optically, gajardoite is uniaxial (–) with ω = 1.780(3) and ε = 1.570(5) (measured in white light). The mineral is nonpleochroic.

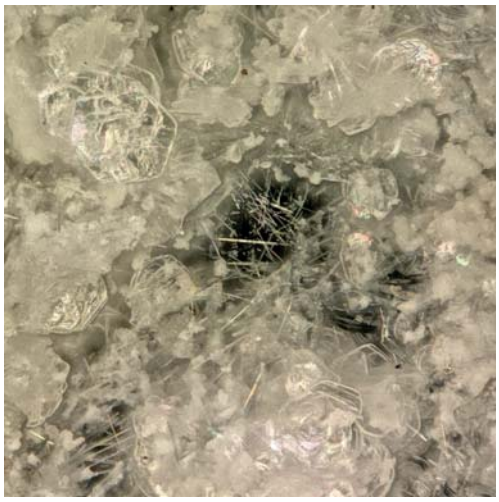

FIG. 1. Gajardoite plates with torrecillasite needles. Field of view 0.7 mm across.

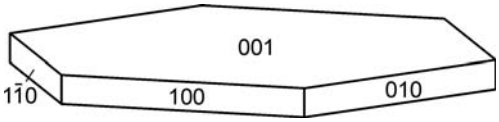

FIG. 2. Crystal drawing of gajardoite, clinographic projection in standard orientation.

Composition

Quantitative analyses (6) were performed at the University of Utah using a Cameca SX-50 electron microprobe with four wavelength-dispersive spectrometers utilizing *Probe for EPMA* software. Analytical conditions were 15 kV accelerating voltage, 10 nA beam current and a beam diameter of 5 μm. Gajardoite was an extremely challenging mineral to analyse. Crystal intergrowths on a very fine scale did not take a good polish and only very narrow areas could be analysed requiring the 5 μm beam diameter. Gajardoite exhibited visible beam damage under the electron beam. Sodium, K and Cl experienced a time-dependent decrease in intensity under the electron beam that was accounted for by an exponential fit to the intensity *vs*. time measurements and extrapolation to zero-time intensity.

No other elements were detected by energy-dispersive spectroscopy. Other probable elements were sought, but none were above the detection limits. Raw X-ray intensities were corrected for matrix effects with a $\phi(\rho z)$ (PAP) algorithm (Pouchou and Pichoir, 1991). The high analytical total is attributed to partial dehydration under vacuum either during carbon coating or in the microprobe chamber. This H_2O loss results in higher concentrations for the remaining constituents than are to be expected for the fully hydrated phase. Because insufficient material was available for a direct determination of H_2O, the amount of water was calculated on the basis of As = 4 atoms per formula unit (apfu), charge balance and O = 11 apfu, as determined by the crystal structure analysis (see below). Analytical data are given in Table 1.

The empirical formula is $(K_{0.77}Ca_{0.71}Na_{0.05}Mg_{0.05})_{\Sigma 1.58}As_4O_{11}Cl_{1.96}H_{9.62}$. The simplified structural formula is $KCa_{0.5}As_4^{3+}O_6Cl_2 \cdot 5H_2O$, which requires K_2O 7.65, CaO 4.55, As_2O_3 64.25, Cl 11.51, H_2O 14.63, O=Cl –2.60, total 100 wt.%. The Gladstone-Dale compatibility $1 - (K_p/K_c)$ for the empirical formula is –0.044 and for

TABLE 1. Analytical data (wt.%) for gajardoite.

Constituent	Mean	Range	SD	Standard
Na_2O	0.26	0.11–0.42	0.10	albite
K_2O	6.13	5.85–6.44	0.22	sanidine
MgO	0.32	0.20–0.43	0.09	diopside
CaO	6.67	6.52–6.87	0.12	diopside
As_2O_3	66.55	62.44–68.49	2.44	syn. GaAs
Cl	11.66	11.44–12.01	0.21	tugtupite
H_2O*	14.58			
O=Cl	–2.63			
Total	103.54			

* Calculated on the basis of As = 4 apfu, charge balance and O = 11 apfu.

the ideal formula is –0.040, both in the range of good compatibility (Mandarino, 2007).

X-ray crystallography and structure refinement

Both powder and single-crystal X-ray studies were carried out using a Rigaku R-Axis Rapid II curved imaging plate microdiffractometer, with monochromatic Mo*K*α radiation. For the powder-diffraction study, a Gandolfi-like motion on the φ and ω axes was used to randomize the sample and observed d-values and intensities were derived by profile fitting using *JADE 2010* software (Materials Data, Inc.). The powder data presented in Table 2 show good agreement with the pattern calculated from the structure determination. Unit-cell parameters refined from the powder data using *JADE 2010* with whole pattern fitting are a = 5.2592(10), c = 15.971(4) Å and V = 382.56(17) Å^3.

The *Rigaku CrystalClear* software package was used for processing structure data, including the application of an empirical absorption correction using *ABSCOR* (Higashi, 2001). The structure was solved by direct methods using *SIR2011* (Burla *et al.*, 2012). *SHELXL-2013* (Sheldrick, 2015) was used for the refinement of the structure. A difference-Fourier synthesis failed to locate the H atom positions. Data collection and refinement details are given in Table 3, atom coordinates and displacement parameters in Table 4, selected bond distances in Table 5 and a bond-valence analysis in Table 6.

The OW2 site was somewhat problematic. With its occupancy and anisotropic displacement parameters refined, it has an occupancy of 0.64(4) and U_{eq} of 0.158(16) Å^2, more than 5x that of the OW3 site. If its U_{iso} is fixed at 0.03, its occupancy refines to only 0.35(2), the Ca site is affected adversely in that its anisotropic displacement parameters become unreasonably small, 0.002(6), and R_1 increases to 0.047. Even fixing the occupancy of the OW2 site at 0.5 and refining its anisotropic displacement parameters, results in a U_{eq} of only 0.008(4) for the Ca site. It is not clear whether the high U_{eq} for the OW2 site implies a lower occupancy or simply a high degree of thermal motion. Ultimately, we decided to report the structure

TABLE 2. Powder X-ray data for gajardoite.

I_{obs}	d_{obs}	d_{calc}	I_{calc}	$h\ k\ l$	I_{obs}	d_{obs}	d_{calc}	I_{calc}	$h\ k\ l$
100	16.00	15.9666	100	0 0 1	3	1.7893	1.7741	1	0 0 9
8	7.94	7.9833	7	0 0 2			1.7296	5	2 0 6
48	5.31	5.3222	29	0 0 3	14	1.7267	1.7226	3	1 1 7
11	4.550	4.5517	5	1 0 0			1.7204	1	2 1 0
8	4.393	4.3773	5	1 0 1			1.7105	1	2 1 1
7	3.978	3.9917	4	0 0 4			1.6530	2	1 0 9
		3.9541	1	1 0 2	9	1.6391	1.6370	5	2 1 3
31	3.466	3.4592	21	1 0 3	6	1.5820	1.5799	5	2 1 4
44	3.013	3.0011	23	1 0 4			1.5172	4	3 0 0
		2.6611	2	0 0 6	13	1.5132	1.5104	1	3 0 1
51	2.624	2.6279	22	1 1 0			1.5005	2	2 0 8
		2.5930	5	1 1 1			1.4905	1	3 0 2
11	2.498	2.4961	5	1 1 2			1.4704	5	1 1 9
36	2.353	2.3563	19	1 1 3	17	1.4605	1.4591	4	3 0 3
		2.2973	4	1 0 6			1.4447	2	2 1 6
3	2.288	2.2809	1	0 0 7			1.3992	2	2 0 9
		2.2758	1	2 0 0			1.3704	1	3 0 5
		2.1886	1	2 0 2			1.3645	2	1 1 10
6	2.0929	2.0925	4	2 0 3			1.3306	1	0 0 12
4	2.0231	2.0291	2	1 1 5			1.3180	3	3 0 6
		1.9771	1	2 0 4	15	1.3133	1.3140	4	2 2 0
21	1.8647	1.8698	11	1 1 6			1.3095	1	2 2 1
		1.8533	1	2 0 5			1.3071	1	2 0 10
		1.8278	2	1 0 8					

TABLE 3. Data collection and structure refinement details for gajardoite.

Diffractometer	Rigaku R-Axis Rapid II
X-ray radiation/power	Mo$K\alpha$ (λ = 0.71075 Å)/50 kV, 40 mA
Temperature	293(2) K
Structural Formula	$K_{0.83}Ca_{0.55}As_4^{3+}O_6Cl_2 \cdot 4.8H_2O$
Space group	*P6/mmm*
Unit cell dimensions	a = 5.2558(8) Å
	c = 15.9666(18) Å
V	381.96(13) Å^3
Z	1
Density (for above formula)	2.599 g/cm^3
Absorption coefficient	9.469 mm^{-1}
F(000)	279.2
Crystal size (μm)	40 × 40 × 2
θ range (°)	3.83 to 25.00
Index ranges	$-5 \le h \le 5$, $-5 \le k \le 6$, $-18 \le l \le 18$
Refls collected / unique	1860 / 189; R_{int} = 0.0685
Reflections with $F_o > 4\sigma(F)$	169
Completeness to θ = 25.00°	99.0%
Max. and min. transmission	0.98 and 0.71
Refinement method	Full-matrix least-squares on F^2
Parameters / restraints	24/0
Goof	1.045
Final R indices [$F_o > 4\sigma(F)$]	R_1 = 0.0349, wR_2 = 0.0708
R indices (all data)	R_1 = 0.0419, wR_2 = 0.0737
Largest diff. peak / hole	+0.67/–0.42 e/A^3

$R_{int} = \Sigma|F_o^2 - F_o^2(\text{mean})|/\Sigma[F_o^2]$. Goof = $S = \{\Sigma[w(F_o^2 - F_c^2)^2]/(n-p)\}^{1/2}$. $R_1 = \Sigma||F_o| - |F_c||/\Sigma|F_o|$. $wR_2 = \{\Sigma[w(F_o^2 - F_c^2)^2]/\Sigma[w(F_o^2)^2]\}^{1/2}$; $w = 1/[\sigma^2(F_o^2) + (aP)^2 + bP]$ where a is 0.0250, b is 4.0431 and P is $[2F_c^2 + \text{Max}(F_o^2, 0)]/3$.

refinement with the occupancy and anisotropic displacement parameters of the OW2 site refined, as that resulted in significantly lower R values and more reasonable displacement parameters for the Ca site. It seems clear that there is a significant amount of disorder in this portion of the structure.

Description of the structure

The structure of gajardoite contains two types of layers (Figs 3 and 4). One layer is made up of two neutral As_2O_3 sheets, between which are K^+ cations and outside of which are Cl^- anions. The As_2O_3

TABLE 4. Atom coordinates and displacement parameters (Å^2) for gajardoite.

	x/a	y/b	z/c	U_{eq}	U^{11}	U^{22}	U^{33}	U^{23}	U^{13}	U^{12}
K*	0	0	1/2	0.030(3)	0.029(3)	0.029(3)	0.033(5)	0	0	0.0147(16)
Ca*	2/3	1/3	0	0.012(4)	0.016(5)	0.016(5)	0.005(7)	0	0	0.008(3)
As	1/3	2/3	0.33634(7)	0.0136(4)	0.0092(5)	0.0092(5)	0.0226(7)	0	0	0.0046(2)
O1	1/2	1/2	0.3966(4)	0.0153(14)	0.013(3)	0.013(3)	0.022(3)	0	0	0.007(3)
OW2*	1/2	0	0.1089(13)	0.158(16)	0.19(3)	0.17(3)	0.103(19)	0	0	0.085(15)
OW3	0	0	0	0.029(5)	0.042(8)	0.042(8)	0.002(8)	0	0	0.021(4)
Cl	0	0	0.2472(3)	0.0287(11)	0.0231(15)	0.0231(15)	0.040(3)	0	0	0.0116(8)

* Occupancies: K: 0.83(2), Ca: 0.273(15), OW2: 0.63(4).

TABLE 5. Selected bond distances (Å) for gajardoite.

As–O1(×3)	1.796(3)
As–Cl(×3)	3.352(2)
K–O1(×12)	3.104(3)
Ca–OW2(×6)	2.308(15)
Hydrogen bonds	
OW3–OW2	3.151(5)
OW2–Cl	3.432(13)
OW3–Cl	3.947(5)

sheets are formed by AsO_3 pyramids connected by shared O atoms (O1). The O atoms in adjacent layers point towards one another and form bonds with the K^+ cations between the sheets. The As apices of the AsO_3 pyramids point away from the centre of the layer, towards peripheral Cl^- anions, with which they form bonds. The ideal formula for this layer is $KAs_4^{3+}O_6Cl_2$.

The second layer consists of an edge-sharing sheet of $Ca(H_2O)_6$ trigonal pyramids with isolated H_2O groups centred in the hexagonal cavities in the sheet. The isolated H_2O groups (OW2) form

TABLE 6. Bond-valence analysis for gajardoite. Values are expressed in valence units (vu).

	O1	OW2	OW3	Cl	Σ_c
K	0.06 ×2↓ 0.07 ×12→				0.84
Ca		0.40 ×6→ 0.11 ×2↓			2.40
As	0.98 ×2↓ 0.98 ×3→			0.04 ×3→ 0.04 ×6↓	3.06
Σ_a	2.08	0.22	0.00	0.24	

Multiplicities indicated by ×↓→; bond strengths based upon assigned site occupancies; K^+–O bond-valence parameters are from Wood and Palenik (1999); Ca^{2+}–O and As^{3+}–O bond strengths from Brown and Altermatt (1985); As^{3+}–Cl bond strengths from Brese and O'Keeffe (1991). Hydrogen bond contributions are not included.

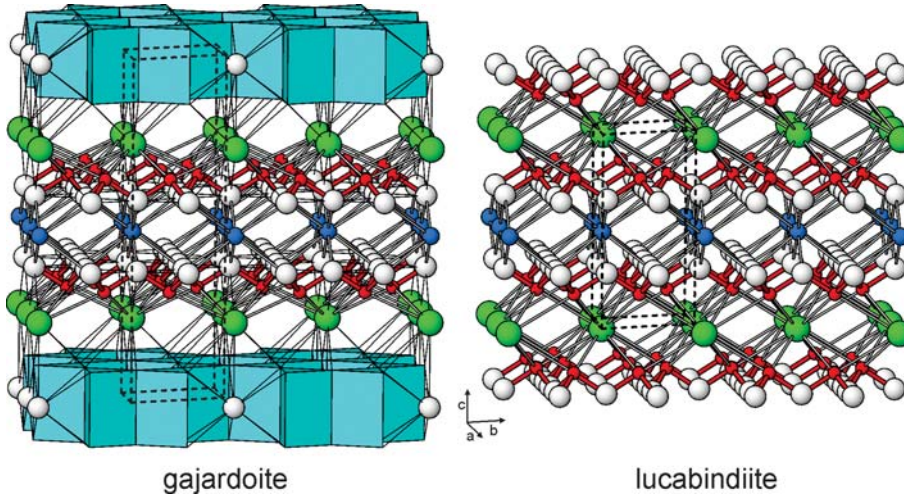

FIG. 3. The crystal structures of gajardoite and lucabindiite. Balls are As (red), K (dark blue), Cl (green) and O (white); $Ca(H_2O)_6$ trigonal pyramids are light blue; sticks are As–O bonds (red) and both As–Cl and K–O bonds (white); thin black lines are hydrogen bonds. The unit cell outlines are shown by dashed black lines.

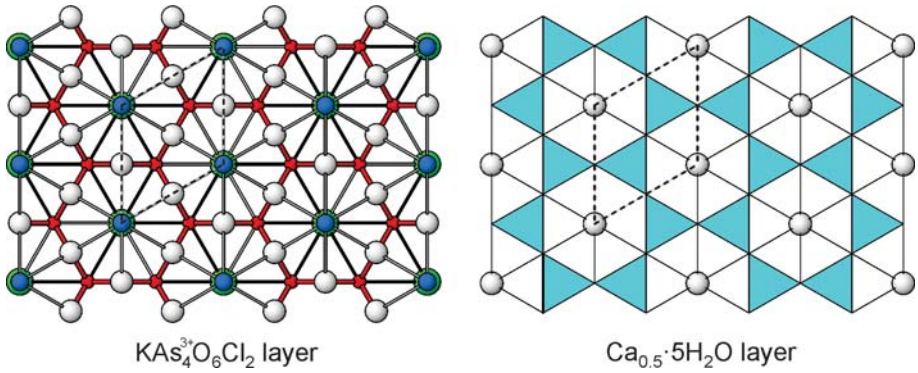

FIG. 4. The $KAs_4^{3+}O_6Cl_2$ layer in gajardoite and lucabindiite, and the $Ca_{0.5}\cdot 5H_2O$ layer in gajardoite, viewed down **c**. Unit cell outlines are shown by dashed black lines.

hydrogen bonds with the O atoms (OW3) of the Ca $(H_2O)_6$ trigonal pyramids and the H_2O groups of the $Ca(H_2O)_6$ trigonal pyramids form hydrogen bonds with the Cl^- anions of the $KAs_4^{3+}O_6Cl_2$ layer. The isolated H_2O groups may also form very long hydrogen bonds with the Cl^- anions. Hence, the two types of layers are joined only by hydrogen bonds. The bond-valence sums (BVS), not including the hydrogen bond contributions, show mostly reasonable values; however, there is one very striking anomaly. The BVS for the Cl site is only 0.24 vu. Interestingly, we note that very low BVS values are found for the Cl site ($Cl_{0.5}Br_{0.3}F_{0.2}$) in lucabindiite (0.31 vu) and the Cl site in torrecillasite (0.49 vu). The very low BVS values for the Cl sites in these structures is probably related to the strong repulsive effects of the As^{3+} lone-pair electrons, which are directed into the interlayer space surrounding the Cl sites. However, it is also likely that the bond-valence parameters for As^{3+}–Cl bonds are in need of revision.

The occupancy of the K site refines to 0.83(2), reasonably close to 0.77 apfu provided by the empirical formula. The occupancy of the Ca site refines to 0.273(15), which yields 0.55 Ca apfu. This is significantly lower than 0.71 apfu provided by the empirical formula; however, it is possible that a small amount of Ca may occupy the K site. Note also that the relatively short Ca–OW2 bond lengths (2.308 Å) and the high BVS (2.40 vu) for the Ca site suggest that the small amounts of Na and Mg indicated in the chemical analyses are accommodated in the Ca site.

The $KAs_4^{3+}O_6Cl_2$ layer in the structure of gajardoite is identical topologically to a slice of the lucabindiite structure (Figs 3 and 4; Garavelli *et al*., 2013) and is similar to, but not topologically identical to, a slice of the torrecillasite structure (Kampf *et al*., 2014*a*).

Acknowledgements

Reviewers Peter Leverett and Anna Garavelli are thanked for their constructive comments on the manuscript. A portion of this study was funded by the John Jago Trelawney Endowment to the Mineral Sciences Department of the Natural History Museum of Los Angeles County.

References

Brese, N.E. and O'Keeffe, M. (1991) Bond-valence parameters for solids. *Acta Crystallographica*, **B47**, 192–197.

Brown, I.D. and Altermatt, D. (1985) Bond-valence parameters from a systematic analysis of the inorganic crystal structure database. *Acta Crystallographica*, **B41**, 244–247.

Burla, M.C., Caliandro, R., Camalli, M., Carrozzini, B., Cascarano, G.L., Giacovazzo, C., Mallamo, M., Mazzone, A., Polidori, G. and Spagna, R. (2012) *SIR2011*: a new package for crystal structure determination and refinement. *Journal of Applied Crystallography*, **45**, 357–361.

Cameron, E.M., Leybourne, M.I. and Palacios, C. (2007) Atacamite in the oxide zone of copper deposits in northern Chile: involvement of deep formation waters? *Mineralium Deposita*, **42**, 205–218.

Garavelli, A., Mitolo, D., Pinto, D. and Vurro, F. (2013) Lucabindiite, $(K,NH_4)As_4O_6(Cl,Br)$, a new fumarole mineral from the "La Fossa" crater at Vulcano, Aeolian Islands, Italy. *American Mineralogist*, **98**, 470–477.

Gutiérrez, H. (1975) *Informe sobre una rápida visita a la mina de arsénico nativo, Torrecillas.* Instituto de Investigaciones Geológicas, Iquique, Chile

Higashi, T. (2001) *ABSCOR.* Rigaku Corporation, Tokyo.

Kampf, A.R., Sciberras, M.J., Williams, P.A., Dini, M. and Molina Donoso, A.A. (2013*a*) Leverettite from the Torrecillas mine, Iquique Provence, Chile: the Co-analogue of herbertsmithite *Mineralogical Magazine*, **77**, 3047–3054.

Kampf, A.R., Nash, B.P., Dini, M. and Molina Donoso, A.A. (2013*b*) Magnesiokoritnigite, $Mg(AsO_3OH)\cdot H_2O$, from the Torrecillas mine, Iquique Province, Chile: the Mg-analogue of koritnigite. *Mineralogical Magazine*, **77**, 3081–3092.

Kampf, A.R., Sciberras, M. J., Leverett, P., Williams, P.A., Malcherek, T., Schlüter, J., Welch, M.D., Dini, M. and Molina Donoso, A.A. (2013*c*) Paratacamite-(Mg), $Cu_3(Mg,Cu)Cl_2(OH)_6$: a new substituted basic copper chloride mineral from Camarones, Chile. *Mineralogical Magazine*, **77**, 3113–3124.

Kampf, A.R., Nash, B.P., Dini, M. and Molina Donoso, A. A. (2014*a*) Torrecillasite, $Na(As,Sb)_4^{3+}O_6Cl$, a new mineral from the Torrecillas mine, Iquique Province, Chile: description and crystal structure. *Mineralogical Magazine*, **78**, 747–755.

Kampf, A.R., Mills, S.J., Hatert, F., Nash, B.P., Dini, M. and Molina Donoso, A.A. (2014*b*) Canutite, $NaMn_3[AsO_4][AsO_2(OH)_2]$, a new protonated alluaudite-group mineral from the Torrecillas mine, Iquique Province, Chile. *Mineralogical Magazine*, **78**, 787–795.

Kampf, A.R., Nash, B., Dini, M. and Molina Donoso, A.A. (2015) Gajardoite, IMA 2015-040. CNMNC Newsletter No. 26, August 2015, page 947; *Mineralogical Magazine*, **79**, 941–947.

Kampf, A.R., Nash, B.P., Dini, M. and Molina Donoso, A.A. (2016) Chongite, $Ca_3Mg_2(AsO_4)_2(AsO_3OH)_2\cdot 4H_2O$, a new arsenate member of the hureaulite group from the Torrecillas mine, Iquique Province, Chile. *Mineralogical Magazine,* **80**, 1255–1263.

Mandarino, J.A. (2007) The Gladstone–Dale compatibility of minerals and its use in selecting mineral species for further study. *The Canadian Mineralogist*, **45**, 1307–1324.

Mortimer, C., Saric, N. and Cáceres, R. (1971) *Apuntes sobre algunas minas de la región costera de la provincia de Tarapacá.* Instituto de Investigaciones Geológicas, Santiago de Chile, Chile.

Pimentel, F. (1978) *Proyecto Arsenico Torrecillas.* Instituto de Investigaciones Geológicas, Iquique, Chile.

Pouchou, J.-L. and Pichoir, F. (1991) Quantitative analysis of homogeneous or stratified microvolumes applying the model 'PAP.' Pp. 3l–75 in: *Electron Probe Quantitation* (K.F.J. Heinrich and D.E. Newbury, editors). Plenum Press, New York.

Sheldrick, G.M. (2015) Crystal structure refinement with SHELXL. *Acta Crystallographica*, **C71**, 3–8.

Wood, R.M. and Palenik, G.J. (1999) Bond valence sums in coordination chemistry using new R_0 values. *Potassium-oxygen complexes. Inorganic Chemistry*, **38**, 1031–1034.